Three-dimensional simulation of downburst winds

Matthew S. Mason[1], Graeme S. Wood[2], David F. Fletcher[3]

[1]*School of Civil Engineering, The University of Sydney*
[2]*Cermak Peterka Peterson, St. Peters, NSW*
[3]*School of Chemical and Biomolecular Engineering, The University of Sydney*

Abstract

Three-dimensional numerical simulations of downburst winds were performed for flow over a flat surface and over an escarpment feature. Simulations with and without downdraft translation and/or environmental cross-flow were performed. It was found that the inclusion of environmental cross-flow inclined the downdraft wind vectors which led to asymmetric velocity fields. For simulations with the topographic features it was found that irrespective of the environmental or translational parameters assumed the speed-up of winds above the crest were less than observed in simulated synoptic boundary layer winds.

Introduction

Observational studies have shown that convectively driven wind events are often asymmetric in nature (Fujita 1985; Hjelmfelt 1988; Wilson et al. 1984). Two primary reasons for this asymmetry are the presence of storm translation and/or low-level environmental winds. Orf and Anderson (1999) studied a series of numerically simulated translating downdrafts occurring in unidirectional environmental flow and suggest that for small translational velocities the maximum outflow velocity increases with an increase in translational speed. No information is given on the physical structure (i.e. velocity profiles) of these events, or whether downdraft translation plays a role in governing this structure. Lin et al. (2007) re-ran a number of these cases at higher grid resolution and show that in a normalised sense the u velocity profiles display similar traits for translating and stationary cases, but indicate a decreasing trend in the elevation of occurrence for storm maximum velocities.

The aim of the current investigation is to use relatively high-resolution ($\Delta x = \Delta y = 20$ m) numerical simulations to simulate the near-ground flow characteristics of stationary and translating downburst events. Translating downdrafts occurring within unidirectional environmental flow, as well as stationary downdrafts with and without unidirectional flow, have been simulated. The simulated cases therefore approximate situations in which a storm system is translating with the environmental flow, the case where environmental winds exist exclusively in the sub-cloud environment, and the baseline case where a stationary storm produces an isolated axi-symmetric outflow. All cases are historically well reported (Fujita 1985; Hjelmfelt 1988; Wilson et al. 1984).

Numerical model description

A non-hydrostatic sub-cloud model was used in a dry three-dimensional mirror-symmetric domain 10 km long, 4 km deep, and 5 km wide. The incompressible continuity, momentum, and energy (potential temperature, θ) equations were solved in the anelastic flux form. The downdraft is initiated by a thermal sink in the energy equation that approximates the evaporative cooling process that occurs when rain/hail falls through a deep, dry, sub-cloud region of a high based thunderstorm. This method is similar to that used by Orf and Anderson (1999). The simplification of microphysical behaviour employed has been used by several authors

successfully (e.g., Krueger and Wakimoto 1985; Mitchell and Hovermale 1977) in order to reduce computational expense while still producing realistic outflow events. However, Mitchell and Hovermale (1977) highlight that this method only simulates the evaporation of precipitation and/or the drag of liquid water in the restricted sense that it produces a positive density anomaly. This therefore means that simulations utilising this forcing method are inherently idealised. This must be appreciated when interpreting the current simulation results.

A neutral lapse rate (dry adiabatic) and a surface temperature of 30°C were prescribed as the reference state for all simulations. This combination led to a melting level of approximately 3 km. A surface roughness parameter of $z_0 = 0.02$ m (open terrain) was used for all simulations, and the corresponding steady-state boundary layer velocity field was set as an initial condition for cases utilising environmental winds. The steady state boundary layer wind field was determined in a separate simulation where no downdraft was initiated. The model equations were closed using the SAS closure scheme (Menter and Egorov 2005), which allowed dynamic length scale calculations in unsteady regions of the flow.

Results and discussion

The simulated downburst event tested are summarised in Table 2. u_{cross} is the environmental cross-flow velocity (at the centre of the forcing function, $z = 2$ km), and u_{trans} is the translational speed of the forcing function.

Table 2 simulated downburst test summaries

Test name	u_{cross} [m/s]	u_{trans} [m/s]	Topography tested
Stationary	0	0	Yes
C18T18	18	18	Yes
C10T18	10	18	No
C18	18	0	Yes
C10	10	0	No

Flow field

Fig. 1 shows the velocity structure along the vertical mirror symmetry plane at the time of maximum storm velocity, u_{storm}, for the three simulations, stationary, C18T18, and C18. Velocity contours and vectors are both shown with contours at $0.1u_{storm}$ intervals. The symmetric nature of the stationary outflow is evident with u_{storm} occurring approximately 1.25 km from the downdraft centre as the burst front begins to diverge from the downdraft. In contrast the C18T18 simulation results show a distinctly asymmetric velocity field with near-ground velocities on the forward side of the outflow significantly larger than those at the rear. For this simulation the velocity contours again indicate a vertical downdraft region of high winds, however inspecting the velocity vectors within the downdraft it is seen that the flow is in fact tilted with respect to the vertical. This behaviour shifts the high pressure dome associated with impingement towards the rear of the downdraft and hence distributes more flow forward. The small magnitude of the rear side outflow is further reduced due to the fact that it must work against the environmental cross-flow. Inspecting the flow field of the C18 simulation it is evident that the presence of environmental cross-flow significantly tilts the downdraft shaft in a manner similar to that reported for many of the JAWS microbursts (Hjelmfelt 1988). A distinct asymmetry is again observed in the near-ground flow with high wind speeds again associated with the forward side

of the outflow. In all cases u_{storm} is seen to be associated with the frontal region of the flow and was shown to occur shortly after the downdraft touches down.

Velocity structure

Inspecting the instantaneous vertical u velocity profiles at the time and location of u_{storm}, Fig. 2 (a), it is evident that all simulation profiles display similar characteristics, but with varying decay rates above the peak. It is also seen that for the C18 simulation the elevation of maximum winds is raised from $z \approx 15$ m to $z \approx 50$ m. This change in profile was found to occur because the maximum wind speed in this case was located towards the front of the diverging burst front, where it is evident from Fig. 1 (c) that the high wind speed region is raised from the surface. The velocity structure of C10 was however seen to have a velocity profile similar to C18T18 due to the similar incidence angles of the downdraft velocity vectors. By the same reasoning the similar behaviour of C10T18 and the stationary case can be explained. Enveloped (maximum at a given elevation throughout the domain for the entire storm event) velocity profiles, Fig. 2 (b), for the same simulations show similar relationships between profiles as discussed for Fig. 2 (a) but with more uniformity above the peak. The changing velocity structure for different simulated events could cause significantly different loading cases for a structure.

Influence of topography

For the test cases shown in Table 2, simulations with escarpment features were tested for normalised slopes of $\phi = 0.2$ and $\phi = 0.5$ (Standards Australia 2002). The escarpment in each case was H = 50 m high and located at the position of u_{storm}. Fig. 3 shows the topographic multiplier profiles (Standards Australia 2002) for the stationary, C18T18, and C18 simulations and compares the results with 2D axi-symmetric simulations conducted previously by the authors, impinging jet results, and numerical boundary layer wind tunnel results at a similar grid resolution. Results for escarpment slopes of $\phi = 0.2$ and $\phi = 0.5$ are shown in Fig. 3 (a) and (b), respectively. It is evident that a good replication of the axi-symmetric results is seen for the three-dimensional stationary simulations, both being slightly lower than the impinging jet results. For the C18T18 and C18 simulations M_t profiles similar in shape to the stationary case are seen but with an offset of approximately 0.1 – 0.2 at all elevations. It is believed that this offset occurs because the presence of the environmental cross-flow helps to confine the movement of the relatively thin diverging wall jet. When comparing the current simulation results with the boundary layer tests, it is however evident that in all cases the velocity speed-up is less.

Conclusions

Three-dimensional downburst simulations were performed to determine the near-ground velocity structure for a number of outflow cases. It was found that the inclusion of environmental cross-flow into simulations inclined the downdraft wind vectors which led to asymmetric velocity fields with a high wind speed bias to the forward side of the outflow. For simulations that included topographic features, it was found that irrespective of the environmental or translational parameters tested the speed-up of winds found above the crest of an escarpment feature were less than observed for simulated boundary layer winds.

References

Fujita, T. T. (1985). "The Downburst: Microburst and Macroburst." *210*, The University of Chicago, Chicago.

Hjelmfelt, M. R. (1988). "Structure and Life Cycle of Microburst Outflows Observed in Colorado." *Journal of Applied Meteorology*, 27(8), 900-927.

Krueger, S. K., and Wakimoto, R. M. "Numerical simulation of dry microbursts." *14th Conference on Severe Local Storms*, Indianapolis, 163-166.

Lin, W. E., Orf, L. G., Savory, E., and Novacco, C. (2007). "Proposed large-scale modelling of the transient features of a downburst outflow." *Wind and Structures, An International Journal*, 10(4), 315-346.

Menter, F. R., and Egorov, Y. (2005). "A Scale-Adaptive Simulation model using two-equation models." 43rd AIAA Aerospace Science Meeting and Exhibit, Paper AIAA 2005-1095, Reno, Nevada.

Mitchell, K. E., and Hovermale, J. B. (1977). "A Numerical Investigation of the Severe Thunderstorm Gust Front." *Monthly Weather Review*, 105(5), 657-675.

Orf, L. G., and Anderson, J. R. (1999). "A Numerical Study of Traveling Microbursts." *Monthly Weather Review*, 127(6), 1244-1258.

Standards Australia. (2002). *AS/NZS 1170.2:2002: Structural design actions. Part 2: Wind actions*, Standards Australia, Sydney.

Wilson, J. W., Roberts, R. D., Kessinger, C., and McCarthy, J. (1984). "Microburst Wind Structure and Evaluation of Doppler Radar for Airport Wind Shear Detection." *Journal of Applied Meteorology*, 23(6), 898-915.

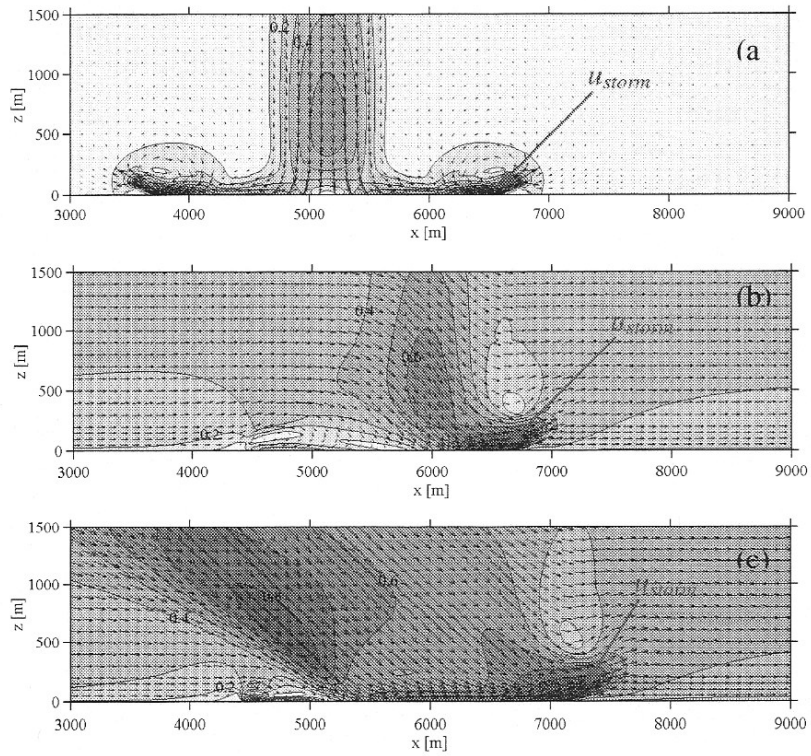

Fig. 1 *U* velocity contour and velocity vector plots at the time of u_{storm} for the (a) stationary, (b) u_{trans} = 18 m/s, u_{cross} = 18 m/s, and (c) u_{cross} = 18 m/s, simulation cases.

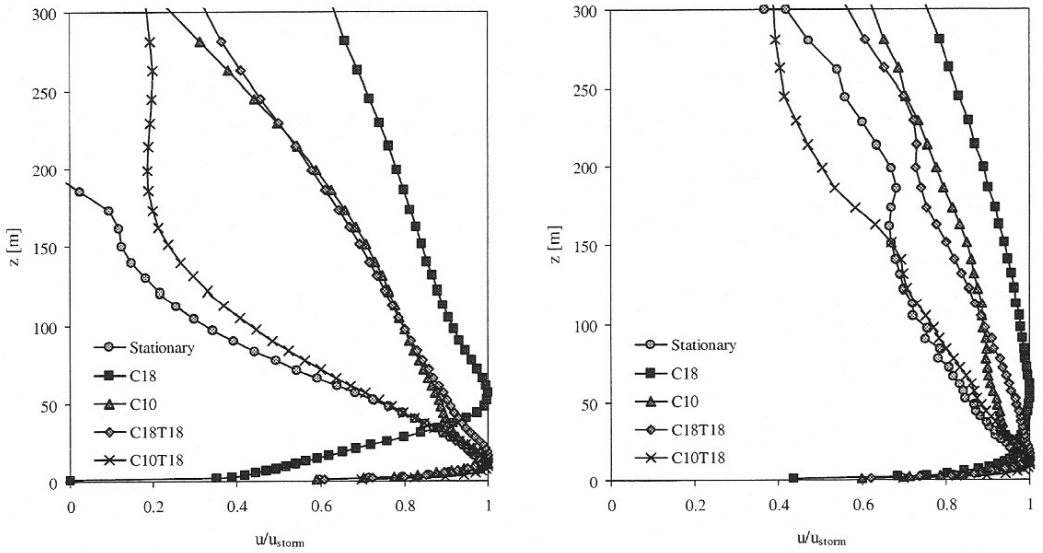

Fig. 2 (a) instantaneous and (b) enveloped u velocity profiles.

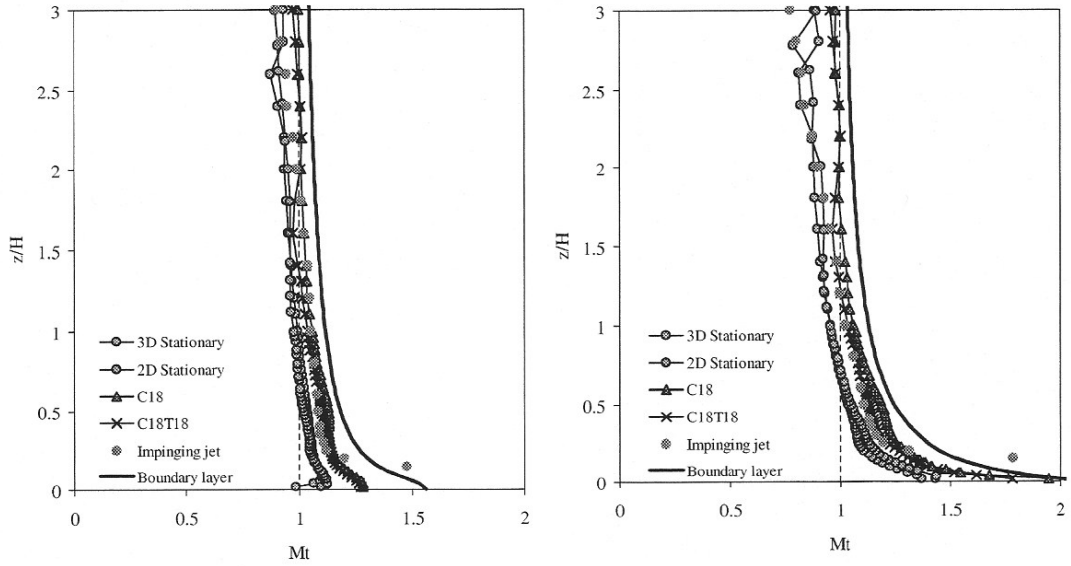

Fig. 3 u velocity envelope topographic multiplier profiles over an escarpment for (a) $\phi = 0.2$, and (b) $\phi = 0.5$.